AGU PUBLICATIONS

Geophysical Research Letters

RESEARCH LETTER

10.1002/2014GL061818

Key Points:
- Martian dynamo can be terminated by impact-induced thermal heterogeneity
- Magnetic field morphology remains intact
- Martian dynamo timing places a lower bound on paleopolar reorientation

Correspondence to:
W. Kuang,
Weijia.Kuang-1@nasa.gov

Citation:
Kuang, W., W. Jiang, J. Roberts, and H. V. Frey (2014), Could giant basin-forming impacts have killed Martian dynamo?, *Geophys. Res. Lett.*, *41*, 8006–8012, doi:10.1002/2014GL061818.

Received 11 SEP 2014
Accepted 24 OCT 2014
Accepted article online 29 OCT 2014
Published online 22 NOV 2014

Could giant basin-forming impacts have killed Martian dynamo?

W. Kuang[1], W. Jiang[2], J. Roberts[3], and H. V. Frey[1]

[1]Planetary Geodynamics Laboratory, NASA Goddard Space Flight Center, Greenbelt, Maryland, USA, [2]Science Systems and Applications, Inc., Lanham, Maryland, USA, [3]Johns Hopkins University Applied Physics Laboratory, Laurel, Maryland, USA

Abstract The observed strong remanent crustal magnetization at the surface of Mars suggests an active dynamo in the past and ceased to exist around early to middle Noachian era, estimated by examining remagnetization strengths in extant and buried impact basins. We investigate whether the Martian dynamo could have been killed by these large basin-forming impacts, via numerical simulation of subcritical dynamos with impact-induced thermal heterogeneity across the core-mantle boundary. We find that subcritical dynamos are prone to the impacts centered on locations within 30° of the equator but can easily survive those at higher latitudes. Our results further suggest that magnetic timing places a strong constraint on postimpact polar reorientation, e.g., a minimum 16° polar reorientation is needed if Utopia is the dynamo killer.

1. Introduction

Strong remanent crustal magnetization inferred from magnetometer and electron reflectometer observations on Mars Global Surveyor suggests that Mars had a core dynamo in its early history, which stopped during the Noachian era [*Acuña et al.*, 1999; *Lillis et al.*, 2008]. Over 30 giant Noachian impact basins of diameters >1000 km (exposed and buried) have been identified [*Frey*, 2008]. Based on the strength of postimpact remagnetization in the crustal rocks of these basins, *Lillis et al.* [2008, 2013], for example, suggested that the global magnetic field vanished toward the end of this basin formation sequence. In particular, Acidalia is strongly magnetized, whereas the younger Utopia basin is completely demagnetized, indicating that the dynamo stopped sometime between the two impact events. These results raise the intriguing question of whether the timing of the basins was merely coincidental or the basin-forming impacts caused the death of the Martian dynamo.

Several studies have been made to link these impacts and the energy for dynamo action. For example, *Roberts et al.* [2009] suggested that shock heating of the mantle by basin-forming impacts could retard core-mantle heat flow to a degree unfavorable for core convection, thus terminating the dynamo. *Arkani-Hamed and Olson* [2010], *Arkani-Hamed* [2012], and *Roberts and Arkani-Hamed* [2014] argued that the impact heating of the core and the lateral mixing would result in stable stratification of the core material, thus reducing the buoyancy flux to a level insufficient to sustain an active dynamo for more than 100 Myr.

To interpret the sudden termination (i.e., in a period much shorter than its lifetime) of the Martian dynamo, *Kuang et al.* [2008] argued that the Martian dynamo could be subcritical in its later stage, and perturbations to the heat flux across the core-mantle boundary (CMB) from the impacts could easily tip the delicate balances among the buoyancy force, the Lorentz force and the Coriolis force in the core, and thus destroy the subcritical dynamo instantly.

The above interpretations focus only on one possible scenario that heating of the core by the impacts could reduce the energy to a level below that needed to drive a core dynamo [*Roberts et al.*, 2009; *Arkani-Hamed and Olson*, 2010; *Arkani-Hamed*, 2012]. However, it is also possible that depending on the core properties and impact angles, the impacts may only create a significant thermal heterogeneity in the mantle, not a substantial heating of the entire core [e.g., *Schultz et al.*, 2007; *Ivanov et al.*, 2010].

Previous studies [e.g., *Stanley et al.*, 2008; *Sreenivasan and Jellinek*, 2012] demonstrated that CMB thermal heterogeneity can play a major role in a supercritical Martian dynamo. Since the Martian dynamo could inevitably be subcritical toward its end [*Kuang et al.*, 2008], and since subcritical dynamos differ substantially

from supercritical dynamos [*Sreenivasan and Jones*, 2011], it is necessary to address a very important question: could the impact-induced thermal heterogeneity terminate a subcritical Martian dynamo? The answer will provide an important piece of the puzzle on the ending of the Martian dynamo.

Here we investigate via numerical simulation of subcritical dynamos, whether the lateral heterogeneity, rather than the total magnitude of the impact-induced thermal perturbation, may be sufficient to terminate the dynamo.

2. Approach

We use the same dynamo model as *Kuang et al.* [2008] and *Jiang and Kuang* [2008] but with impact-induced heterogeneous heat flux across the CMB. In this model, the buoyancy force, the fluid viscosity, the magnetic diffusivity, and the thermal conductivity are given by the nondimensional Rayleigh number R_{th}, the Ekman number E, the magnetic Rossby number R_o, and the modified Prandtl number p_κ, respectively. Except R_{th}, the other parameter values are the same as in *Kuang et al.* [2008]. The numerical resolution is much higher, with the maximum 180 spherical harmonic degrees, and 160 radial grid points, but the subcritical dynamo region remains significant: the critical point to terminate a subcritical dynamo is $R_{\mathrm{cr}} \approx 1900$, and the critical point for the onset of the dynamo is $R_{\mathrm{cf}} \approx 2600$.

Impact-induced thermal perturbations in this study follow those of *Roberts et al.* [2009]. The mantle is heated by a shock wave emanating from the impact location at the colatitude θ_l and the longitude ϕ_l on the surface. Assuming that melt production does not consume any waste heat, the shock produces a temperature increment [*Watters et al.*, 2009]

$$\Delta T = \frac{1}{C_p}\left[\frac{\Delta P}{2\rho_0 S}\left(1-\frac{1}{f}\right)-\left(\frac{C}{S}\right)^2\left(f-\ln f-1\right)\right], \tag{1}$$

where ΔP is the difference between the shock pressure P_s and the lithostatic pressure P_0, C and S are the intercept and slope of the equation of state relating the shock and particle velocities, ρ_0 is the mean density, and

$$f = -\frac{2S\Delta P}{C^2\rho_0}\left(1-\sqrt{1+\frac{4S\Delta P}{C^2\rho_0}}\right)^{-1}. \tag{2}$$

The shock pressure P_s and thus ΔT decay rapidly with the distance from the impact center [e.g., *Pierazzo et al.*, 1997]. This ΔT is added to a prevailing temperature field in mantle convection simulation with CitcomS model [*Zhong et al.*, 2000; *Tan et al.*, 2006]. The heat flux perturbations are then derived from both preimpact and postimpact temperature distributions. Mathematically, the postimpact total heat flux, scaled by the uniform mean heat flux h_0, across the CMB can be written as

$$h_T/h_0 = 1+\epsilon_l \delta h\left(\theta,\phi\right) = 1+\epsilon_l \sum_{l,m} h_l^m Y\left(\theta,\phi\right) + C.C., \tag{3}$$

where δh is the normalized impact-induced heat flux perturbation (as shown in Figure 1), ϵ_l is the relative heterogeneity amplitude, and $C.C.$ is the complex conjugate part (to ensure a real heat flux perturbation).

For dynamo simulation, h_T is assumed time invariant, since the dynamo timescales are much shorter than those of mantle convection. For example, the magnetic diffusion time $\tau_\eta \approx 40,000$ years, many orders of magnitude shorter than those of the mantle convection (tens of Myr). Because dynamo solutions are periodic in azimuth (with the z axis as the mean rotation axis), we can also assume without loss of generality that $\phi_l = 0$, i.e., impact locations are specified only via θ_l, which varies from 0° (the north pole) to 90° (the equator). For easier numerical implementation, we divide the total temperature T into two parts:

$$T\left(t,r,\theta,\phi\right) = T_a\left(r,\theta,\phi\right) + \Theta\left(t,r,\theta,\phi\right), \tag{4}$$

where T_a is a steady, conducting distribution with the boundary condition $\left(\partial T_a/\partial r\right)_{\mathrm{CMB}} = -h_T$ and the time varying Θ is solved via the energy equation with the boundary condition $\left(\partial\Theta/\partial r\right)_{\mathrm{CMB}} = 0$. From now on, unless otherwise stated, all quantities are nondimensional.

Survivability of subcritical dynamos with (3) is examined as follows: all simulations start from the same initial state that is a well-established subcritical dynamo solution without the heterogeneity ($\epsilon_l = 0$). This ensures

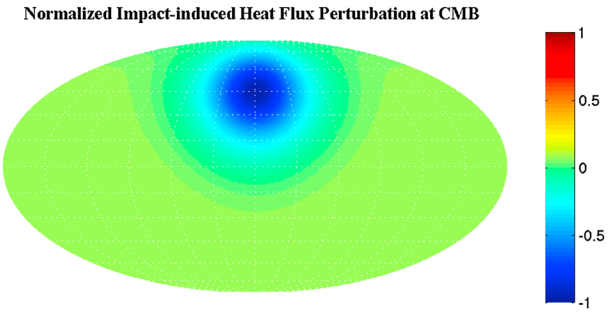

Figure 1. An example of the normalized impact-induced heat flux perturbation δh in (3) at the CMB due to an impact centered at $\theta_l = 45°$. The blue and orange represent the negative and positive heat flux anomaly (relative to the background uniform heat flux) out of the CMB, respectively.

that all subsequent changes of the dynamos are only caused by the implementation of (3). The dynamo is terminated if, to leading order, the RMS field strength

$$B = \left(\frac{1}{V_{\text{core}}} \int_{V_{\text{core}}} |\mathbf{B}|^2 \, dV \right)^{1/2} \tag{5}$$

decays exponentially in time, i.e., $B \sim B_0 e^{-\lambda t}$ ($\lambda > 0$). Otherwise, it survives the impact.

Given an impact location θ_l, the amplitude ϵ_l increases from 0 to a critical value ϵ^c where the subcritical dynamo could no longer be sustained. To be consistent with the Boussinesq approximation in our model, ϵ_l cannot be very large. Thus, we set up an upper limit $\epsilon_l \leq 0.3$ which can account for up to 90% of large basin-forming impacts [see *Roberts et al.*, 2009, Figure 3]. We conclude that within our model capacity, the impact will not kill the subcritical dynamo if $\epsilon^c > 0.3$.

3. Results

The effects of the impact-induced CMB thermal heterogeneity (3) on subcritical dynamos are summarized in Figure 2. In this figure, each circle represents a subcritical dynamo simulation result: filled circles are the dynamos that survived the impacts and the open circles are those disabled by the impacts. The heterogeneity (3) properties define the coordinates: the amplitude ϵ_l is the radius, and the location $\left(90° - \theta_l\right)$ is the polar angle. From the figure one can observe that

$$\epsilon^c > 0.3 \quad \text{if} \quad \left|90° - \theta_l\right| \geq 30°;$$
$$\epsilon^c \leq 0.3 \quad \text{if} \quad \left|90° - \theta_l\right| < 30°.$$

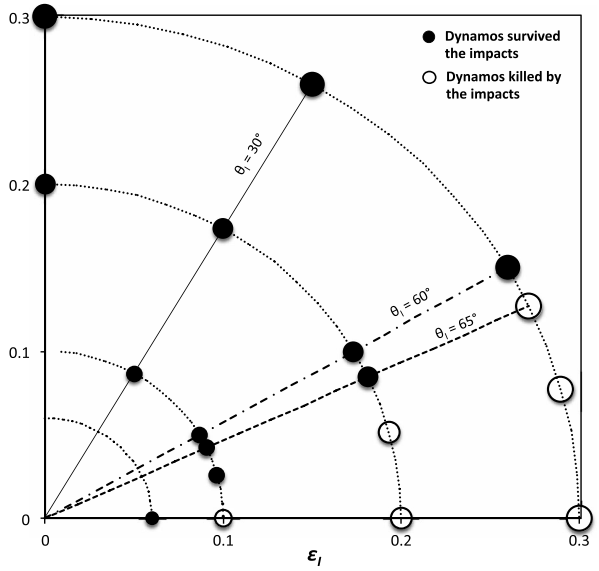

Figure 2. Survivability of subcritical dynamos under the impact-induced thermal heterogeneity (3). The solid circles are the dynamos that survived the impacts, while the open circles are those killed by the impacts. The polar coordinates of the symbols describe the heterogeneity properties: the radius is the relative amplitude ϵ_l of the heterogeneity, and the polar angle is the impact center latitude $(90° - \theta_l)$.

This suggests a critical boundary $\left|90° - \theta_l^c\right| = 30°$: if located outside the boundary, the heterogeneity (3) could not stop the subcritical dynamos; otherwise, it could terminate the dynamos, provided that $\epsilon_l \geq \epsilon^c$. In summary, subcritical dynamos could easily survive the impacts near the polar regions but will be more likely killed by those near the equator. Our findings are similar to some earlier dynamo simulation results. For example, *Sreenivasan and Jellinek* [2012] showed that (supercritical) dynamos are more easily killed by thermal heterogeneity near the equator than near the polar regions.

To better understand how the thermal heterogeneity (3) could terminate a subcritical dynamo, we examine the dynamo field properties and its generation mechanisms.

As shown in Figure 3, the poloidal magnetic field of the subcritical dynamos is hemispherically asymmetric at the CMB: the temporal mean radial component $\overline{B}_r = \left(\int_0^T B_r dt \right) / T$ is very strong in the

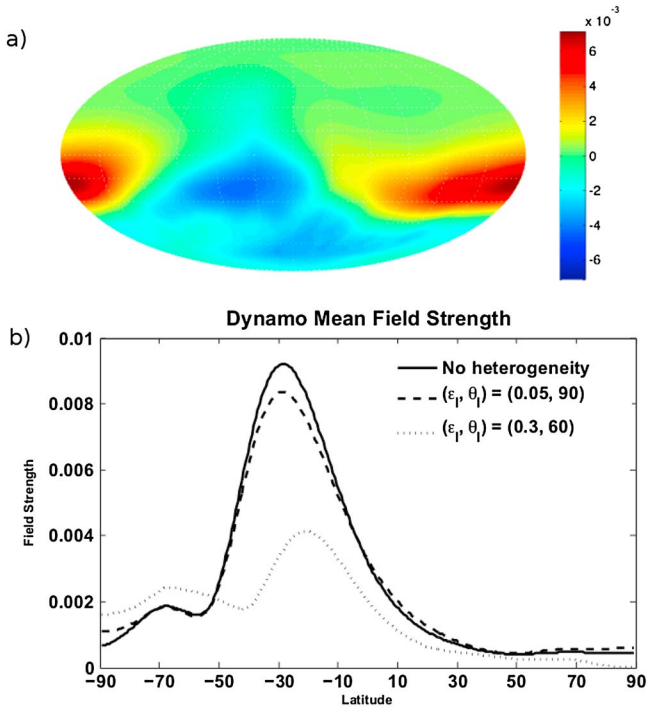

Figure 3. The properties of the radial magnetic field B_r at the CMB: (a) the temporal mean $\overline{B}_r$ with $\epsilon_l = 0.3$ and $\theta_l = 60°$ and (b) the azimuthal RMS field strength $\mathcal{B}_r$ (6) with $\epsilon_l = 0$ (the solid line), $\epsilon_l = 0.05$ and $\theta_l = 0°$ (the dashed line), and $\epsilon_l = 0.3$ and $\theta_l = 60°$ (the dotted line).

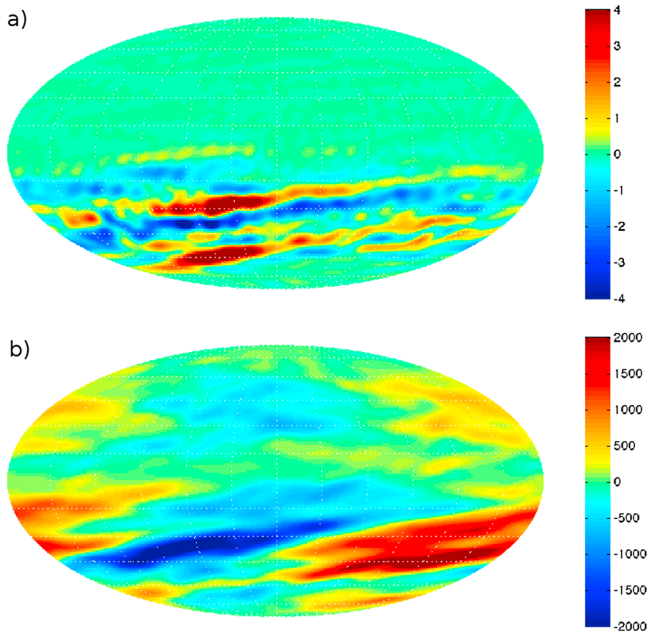

Figure 4. The dynamo action and the helicity of the subcritical dynamo with the heterogeneity $\epsilon_l = 0.05$ and $\theta_l = 90°$: (a) the temporal mean dynamo action $\overline{F}_D$ in midcore and (b) the temporal mean helicity $\overline{H}$ at the same radial position.

southern hemisphere (see Figure 3a), while its latitudinal RMS distribution

$$\mathcal{B}_r(\theta) = \left(\frac{1}{2\pi}\int_0^{2\pi} \overline{B}_r^2 d\phi\right)^{1/2} \quad (6)$$

is nearly an order of magnitude stronger in the southern hemisphere than in the northern hemisphere (Figure 3b). We can also observe from the figure that the thermal heterogeneity (3) reduces significantly the field strength but less so to the hemispherical asymmetry. For example, $\mathcal{B}_r$ with the heterogeneity of $\theta_l = 60°$ and $\epsilon_l = 0.3$ (the dotted line in Figure 3b) is nearly one third of that without heterogeneity (the solid line in the figure). But the latitudinal location of the maximum magnitude is only shifted by approximately 10° toward the equator.

The field hemispherical asymmetry implies that of the dynamo action in the core and can be shown through the magnetic energy variation in the core derived from the magnetic induction

$$\frac{1}{2}\left(\frac{\partial}{\partial t}+\mathbf{v}\cdot\nabla\right)B_r^2 = B_r\left(\mathbf{B}\cdot\nabla\right)v_r + B_r\left(\nabla^2\mathbf{B}\right)_r, \quad (7)$$

where $\mathbf{v}$ is the fluid velocity and v_r is its radial component. Equation (7) shows that the total time variation of the magnetic energy $B_r^2/2$ (the left side) is determined by the dynamo action $F_D \equiv B_r\left(\mathbf{B}\cdot\nabla\right)v_r$ and the Ohmic dissipation $F_\eta \equiv B_r\left(\nabla^2\mathbf{B}\right)_r$. For an active dynamo, $F_D > 0$ in part of the core (hereafter defined as the dynamo region). Because the flow helicity $H \equiv \mathbf{v}\cdot(\nabla\times\mathbf{v})$ is critical for dynamo action [e.g., *Moffatt*, 1978], we analyze F_D and H together.

In Figure 4 we show the temporal means $\overline{F}_D$ and $\overline{H}$ in the midcore with the heterogeneity $\epsilon_l = 0.05$ and $\theta_l = 90°$ (the equator). This figure shows strong hemispherical asymmetries in $\overline{F}_D$ and $\overline{H}$. In addition, both display striking northeast-southwest stripes across midlatitudes, indicating strong correlations between H and F_D. Their latitudinal distributions

$$\left[\mathcal{F}_D, \mathcal{H}\right](\theta) = \sin\theta\int r^2 dr d\phi\left[\overline{F}_D, \overline{H}\right](r,\theta,\phi) \quad (8)$$

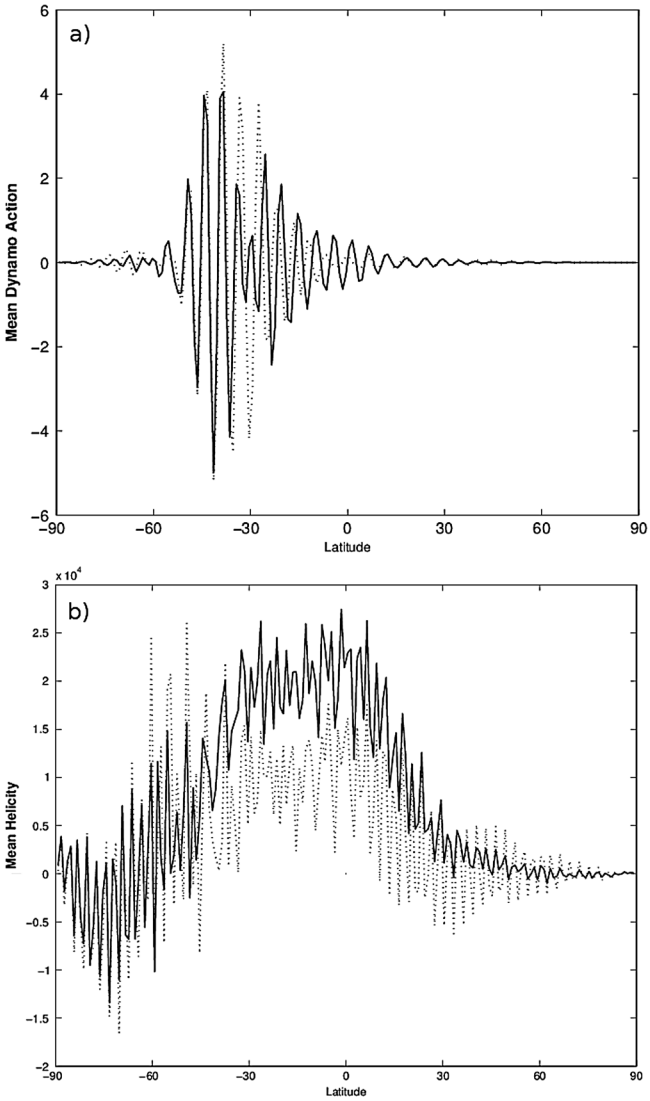

Figure 5. The integrated (a) dynamo action $\mathcal{F}_D$ and (b) the helicity $\mathcal{H}$ defined in (8) of two subcritical dynamos: one without thermal heterogeneity $\epsilon_l = 0$ (the solid lines) and the other with the heterogeneity $\epsilon_l = 0.05$ and $\theta_l = 90°$ (the dotted lines).

are shown in Figure 5. From the figure we observe similar strong hemispherical asymmetries. In particular, as shown in Figure 5b, (3) does not affect much the hemispherical asymmetry but reduces significantly the helicity $\mathcal{H}$ in the core and thus the effectiveness of the dynamo action.

4. Implications for Martian Dynamo History

Our simulation results demonstrate clearly that subcritical dynamos are prone to impact-induced thermal heterogeneity (3) at the CMB, especially those centered near the equator. We examine the implications of our results for the termination of the Martian dynamo by focusing on several known giant impact basins on Mars. For example, as shown by *Lillis et al.* [2008, 2013], the Martian dynamo likely ceased between the formation of Acidalia and Utopia basins: the postimpact remagnetization in the Acidalia basin is likely more than an order of magnitude stronger than that in the Utopia basin. Thus, our results may suggest that Utopia (or an earlier large basin-forming impact) could have killed the dynamo, since the dynamo magnetic decay timescales are much shorter than those of the uppermost crust to cool down below the Curie point of any likely magnetic mineral [*Dunlop and Arkani-Hamed*, 2005].

However, Utopia is currently centered approximately at $\theta_l \approx 46°$. If we consider only the impact-induced thermal heterogeneity, then based on our simulation results that $\theta_l > 60°$ for terminating the subcritical dynamos, it would not be able to kill the Martian dynamo. This could be invalid for two scenarios: either the Utopia impact could have heated up the entire core substantially such that the available buoyancy force is insufficient to drive a subcritical dynamo or a polar reorientation could have occurred after the impact to move the impact center to the current high-latitude location.

The first scenario depends on the impact properties and Martian interior structures. Since the initial heterogeneous heating of the core can be well mixed convectively in a transient period $\tau_t \approx \tau_\eta / R_m$ (e.g., 100 years with a typical magnetic Reynolds number $R_m \approx 400$ in the core [*Kuang et al.*, 2008]), the core heating could be effectively described by a smaller mean heat flux h_0 in (3) across the CMB after τ_t. *Arkani-Hamed and Olson* [2010] found similar horizontal mixing timescales and a much longer lived stably stratified layer at the top of the core. The latter would not change our results qualitatively.

For the second scenario, a lower bound could be obtained from this study. Since the subcritical dynamos will survive an impact more than 30° away from the equator, this suggests that a postimpact 16° northward polar reorientation is necessary for terminating the dynamo by Utopia. It is interesting to note that studies of

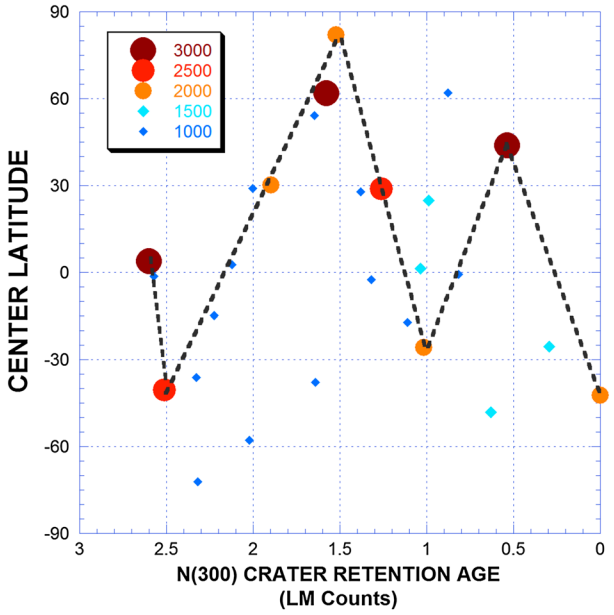

Figure 6. Basin center latitude versus N(300) Crater Retention Age for 30 very large basins on Mars (with diameters larger than 1000 km) [*Frey*, 2008]. Basins larger than 2000 km diameter are shown as large circles. These follow a systematic pattern in their latitudes that could be explained if the very largest impacts tried to reorient Mars by migrating toward the poles and subsequent impacts occurred mostly near the equator.

retention ages [*Frey*, 2008] indicate a systematic sawtooth time variation pattern in the latitudinal locations of the largest basins on Mars (see Figure 6), suggesting postimpact polar reorientations.

It is possible that events other than the large basin-forming impacts could end the Martian dynamo. For example, *Hood et al*. [2005] suggested an even larger polar reorientation from internal mass redistribution associated with, e.g., formation of Tharsis. The Tharsis plateau is younger than the Utopia basin, but its formation could start much earlier. Provided that the Tharsis plume was near the equator, the thermal heterogeneity associated with the plume could also kill the Martian dynamo, as suggested by our results and by *Sreenivasan and Jellinek* [2012]. However, other studies also suggest Tharsis plume migration during its uprising [e.g., *Šrámek and Zhong*, 2012]. These certainly bring additional complications on the cause of the Martian dynamo termination. There are also debates on the timing of the Martian dynamo [*Hood et al.*, 2010]. These may suggest that processes not related to impacts, e.g., reduction of heat flux across the CMB over time, could eventually shut down the dynamo. But this is far beyond the scope of this study.

Regardless, our study finds that subcritical dynamos are very sensitive to small thermal heterogeneity across the CMB. If such heterogeneity kills the Martian dynamo, then the magnetic timing will place a strong constraint on the location of the heterogeneity and on possible polar reorientation of Mars.

Acknowledgments

This research is supported by NASA Mars Fundamental Research Program and by NASA Mars Data Analysis Program. We also thank NASA NAS on high-end scientific computation support. The data (dynamo simulation results) used for this paper are available upon request (weijia.kuang-1@nasa.gov).

Andrew Dombard thanks Robert Lillis and one anonymous reviewer for their assistance in evaluating this paper.

References

Acuña, M. H., et al. (1999), Global distribution of crustal magnetization discovered by the Mars Global Surveyor MAG/ER experiment, *Science*, *35*, 790–793.

Arkani-Hamed, J. (2012), Life of the Martian dynamo, *Phys. Earth Planet. Inter.*, *197*, 83–96.

Arkani-Hamed, J., and P. Olson (2010), Giant impact stratification of the Martian core, *Geophys. Res. Lett.*, *37*, L02201, doi:10.1029/2009GL041417.

Dunlop, D. J., and J. Arkani-Hamed (2005), Magnetic minerals in the Martian crust, *J. Geophys. Res.*, *110*, E12S04, doi:10.1029/2005JE002404.

Frey, H. V. (2008), Ages of very large impact basins on Mars: Implications for the late heavy bombardment in the inner solar system, *Geophys. Res. Lett.*, *35*, L13203, doi:10.1029/2008GL033515.

Hood, L. L., C. N. Young, N. C. Richmond, and K. P. Harrison (2005), Modeling of major Martian magnetic anomalies: Further evidence for polar reorientations during the Noachian, *Icarus*, *177*, 144–173.

Hood, L. L., K. P. Harrison, B. Langlais, R. J. Lillis, F. Poulet, and D. A. Williams (2010), Magnetic anomalies near Apollinaris Patera and the Medusae Fossae formation in Lucus, Planum, Mars, *Icarus*, *208*, 118–131.

Ivanov, B. A., H. J. Melosh, and E. Pierazzo (2010), Basin-forming impacts: Reconnaissance modeling, *Geol. Soc. Am. Spec. Pap.*, *465*, 29–49.

Jiang, W., and W. Kuang (2008), An MPI-based MoSST core dynamics model, *Phys. Earth Planet. Inter.*, *170*, 46–51.

Kuang, W., W. Jiang, and T. Wang (2008), Sudden termination of Martian dynamo?: Implications from subcritical dynamo simulations, *Geophys. Res. Lett.*, *35*, L14204, doi:10.1029/2008GL034183.

Lillis, R. I., H. V. Frey, and M. Manga (2008), Rapid decrease in Martian crustal magnetization in the Noachian era: Implications for the dynamo and climate of early Mars, *Geophys. Res. Lett.*, *35*, L14203, doi:10.1029/2008GL034338.

Lillis, R. I., S. Robbins, M. Manga, J. S. Halekas, and H. V. Frey (2013), Time history of the Martian dynamo from crater magnetic field analysis, *J. Geophys. Res. Planets*, *118*, 1488–1511, doi:10.1002/jgre.20105.

Moffatt, H. K. (1978), *Magnetic Field Generation in Electrically Conducting Fluids*, Cambridge Univ. Press, Cambridge, U. K.

Pierazzo, E., A. M. Vickery, and H. J. Melosh (1997), A reevaluation of impact melt production, *Icarus*, *127*, 408–423.

Roberts, J. H., and J. Arkani-Hamed (2014), Impact heating and coupled core cooling and mantle dynamics on Mars, *J. Geophys. Res. Planets*, *119*, 729–744, doi:10.1002/2013JE004603.

Roberts, J. H., R. I. Lillis, and M. Manga (2009), Giant impacts on early Mars and cession of the Martian dynamo, *J. Geophys. Res.*, *114*, E04009, doi:10.1029/2008JE003287.

Schultz, P. H., C. A. Eberhardy, C. M. Ernst, M. F. A'Hearn, J. M. Sunshine, and C. M. Lisse (2007), The deep impact oblique impact cratering experiment, *Icarus*, *190*, 295–333.

Šrámek, O., and S. Zhong (2012), Martian crustal dichotomy and Tharsis formation by partial melting coupled to early plume migration, *J. Geophys. Res.*, *117*, E01005, doi:10.1029/2011JE003867.

Sreenivasan, B., and A. M. Jellinek (2012), Did the Tharsis plume terminate the Martian dynamo?, *Earth Planet. Sci. Lett.*, *350*, 209–217.

Sreenivasan, B., and C. A. Jones (2011), Helicity generation and subcritical behaviour in rapidly rotating dynamos, *J. Fluid Mech.*, *688*, 5–30.

Stanley, S., L. Elkins-Tanton, M. T. Zuber, and E. M. Parmentier (2008), Mars' paleomagnetic field as the result of a single-hemisphere dynamo, *Science*, *321*, 1822–1825.

Tan, E., E. Choi, P. Thoutireddy, M. Gurnis, and M. Aivazis (2006), GeoFramework: Coupling multiple models of mantle convection within a computational framework, *Geochem. Geophys. Geosyst.*, *7*, Q06001, doi:10.1029/2005GC001155.

Watters, W. A., M. T. Zuber, and B. H. Hager (2009), Thermal perturbations caused by large impacts and consequences for mantle convection, *J. Geophys. Res.*, *114*, E02001, doi:10.1029/2007JE002964.

Zhong, S., M. T. Zuber, L. Moresi, and M. Gurnis (2000), Role of temperature-dependent viscosity and surface plates in spherical shell models of mantle convection, *J. Geophys. Res.*, *105*, 11,063–11,082.